Bioorganic Chemistry 83 (2019) 432–437

Contents lists available at ScienceDirect

Bioorganic Chemistry

journal homepage: www.elsevier.com/locate/bioorg

Synthesis and biological evaluation of pyrano[4,3-*b*][1]benzopyranone derivatives as monoamine oxidase and cholinesterase inhibitors

Koichi Takao*, Yuka Kubota, Hitoshi Kamauchi, Yoshiaki Sugita

Laboratory of Bioorganic Chemistry, Department of Pharmaceutical Sciences, Faculty of Pharmacy and Pharmaceutical Sciences, Josai University, 1-1 Keyaki-dai, Sakado, Saitama 350-0295, Japan

A B S T R A C T

A series of eighteen pyrano[4,3-*b*][1]benzopyranone derivatives (**1a**-**9b**) were synthesized, and structure-activity relationships of their monoamine oxidase (MAO) A and B, acetylcholinesterase (AChE), and butyrylcholinesterase (BChE) inhibitory activities were evaluated. Most of the synthesized compounds exhibited weak inhibitory activity toward MAO-A, whereas compounds **2a**, **2b**, **4a**, **4b**, **5a**, **5b**, **6a**, **6b**, **8a** and **8b** showed potent inhibitory activities toward MAO-B. Intriguingly, compounds **5a**, **5b**, and **8a** showed inhibitory activities comparable to pargylin, used as a positive control for MAO-B. Substitution of butoxy at the C3 position or of chlorine at the C8 position of pyrano[4,3-*b*][1]benzopyranone increased the inhibitory activity of the compound toward MAO-B. The results of a molecular docking study supported this structural effect. Most of the compounds exhibited no or slight inhibitory activity toward AChE and BChE, with *exo* type compounds bearing a butoxy group, such as compounds **2b**, **5b** and **8b**, showing weak but distinct inhibitory activities toward BChE. This report is the first to identify pyrano[4,3-*b*][1]benzopyranone derivatives as potent and selective MAO-B inhibitors. 3-Butoxy-8-chloro-pyrano[4,3-b][1]benzopyranone (**5b**) may be useful as a lead compound for the development of MAO-B inhibitors.

1. Introduction

Alzheimer's disease is the leading cause of dementia, and because the primary risk factor for Alzheimer's disease is old age, the number of affected people is increasing dramatically as the global population ages and is expected to reach 131 million by 2050 [1]. Unfortunately, there is no effective treatment for Alzheimer's disease. Current therapeutic options, which include acetylcholinesterase and butyrylcholinesterase (AChE and BChE) inhibitors (donepezil, rivastigmine, and galantamine), and an NMDA receptor antagonist (memantine), provide modest improvement in memory and cognitive function but are only palliative and do not prevent progressive neurodegeneration. The free radical and oxidative stress theory of aging suggests that oxidative damage is an important factor in neuronal degeneration. Therefore, protecting neuronal cells from oxidative damage could potentially prevent Alzheimer's disease [2].

Monoamine oxidases A and B (EC 1.4.3.4; MAO-A and MAO-B) are flavoenzymes that bind to the mitochondrial outer membranes of various mammalian cell types [3]. MAO-A and MAO-B play an important role in the oxidative degradation of neurotransmitters such as dopamine, serotonin, and epinephrine. MAO-A and MAO-B share approximately 70% sequence identity at the amino acid level and were identified based on their substrate and inhibitor sensitivities. MAO-A preferentially catalyzes the oxidative deamination of serotonin, norepinephrine, and epinephrine, and is irreversibly inhibited by clorgyline. In contrast, MAO-B preferentially deaminates dopamine, 2-phenetylamine, and benzylamine, and is irreversibly inhibited by R-(-)-deprenyl. The administration of MAO inhibitors has a beneficial effect in the treatment of several neurodegenerative diseases [4,5]. There is considerable evidence that MAO-B activity increases in the brain as aging progresses whereas there is no comparable evidence for MAO-A. Furthermore, MAO-B inhibitors such as selegiline and rasagiline have shown efficacy in improving learning and memory deficits in Alzheimer's disease animal models and to slow the progression of Alzheimer's disease in patients. Therefore, selective MAO-B inhibitors would likely be of value for Alzheimer's disease therapy [6–9].

4*H*-1-Benzopyran-4-ones (chromones, 4*H*-1-chromen-4-ones) are an important class of oxygenated heterocyclic compounds that have attracted the attention of organic chemists and biochemists due to their biological activities [10]. The chromone core structure is found in flavones and isoflavones, which are secondary metabolites that are ubiquitous in nature and especially in the plant kingdom and are present in notable amounts in several plant species. 2,3-Dihydro-1-benzopyran-4-ones (chromanones, chroman-4-ones) are an important scaffold structure in drug discovery and development [11]. The chromanone core structure is found in many natural compounds such as flavanones, isoflavanones, and homoisoflavanones [12–14].

Chromone and chromanone scaffolds are the pharmacophores of a

* Corresponding author.
E-mail address: ktakao@josai.ac.jp (K. Takao).

https://doi.org/10.1016/j.bioorg.2018.11.004
Received 15 September 2018; Received in revised form 1 November 2018; Accepted 2 November 2018
Available online 03 November 2018
0045-2068/

large number of bioactive molecules of both natural and synthetic origin. These bioactive molecules have been studied as candidate drugs for treating Alzheimer's disease, such as ChE inhibitors, MAO inhibitors, β-secretase inhibitors and amyloid β aggregation inhibitors [12].

In contrast, there have been few studies on pyrano[4,3-*b*][1]benzopyranones, which are derived from chromones. Although several synthetic studies have been conducted[15–18], only a few studies have evaluated their biological activities[19,20].

In the present study, a series of pyrano[4,3-*b*][1]benzopyranones were synthesized and the structure-activity relationships (SARs) of their MAO and ChE inhibitory activities were investigated in an effort to further the discovery of new compounds useful for treating Alzheimer's disease and to further explore the biological activities of pyrano[4,3-*b*][1]benzopyranones.

2. Results and discussion

2.1. Chemistry

3-Formylchromones behave as heterodienes in hetero Diels-Alder reactions with enol ethers. The pyrano[4,3-*b*][1]benzopyranone derivatives (**1a** - **9b**) were synthesized by cycloaddition reactions of 3-formylchromones (**Ia-c**) with excess selected enol ether (**IIa-c**) according to methods reported previously[15] (Fig. 1).

All products were obtained as a mixture of *endo* and *exo* type adducts. These isomer were determined by the coupling constant between H-3 and H-4α (J ≒ 10 Hz: *endo* adducts, J ≒ 2.5 Hz: *exo* adducts). Yields of *endo* type adducts with higher amount than that of *exo* type (Table 1). Therefore, the structure of *endo* and *exo* type adducts (**3a**, **3b**, **6a**, **6b**, **9a**, **9b**) by using methyl enol ethers were defined by their yields.

2.2. Inhibitory activities of the synthetic compounds toward MAOs

Eighteen pyrano[4,3-*b*][1]benzopyranone derivatives (**1a-9b**) were evaluated for MAO-A and MAO-B inhibitory activity according to the assay methods described in the Experimental section. Most of the compounds showed weak inhibitory activity toward MAO-A, except for compounds **6a** and **8b**, which showed distinct inhibitory activities. In contrast, compounds **2a**, **2b**, **4a**, **4b**, **5a**, **5b**, **6a**, **6b**, **8a** and **8b** showed potent and selective inhibitory activities toward MAO-B. In particular, compounds **5a, 5b,** and **8a** inhibited MAO-B activity most potently,

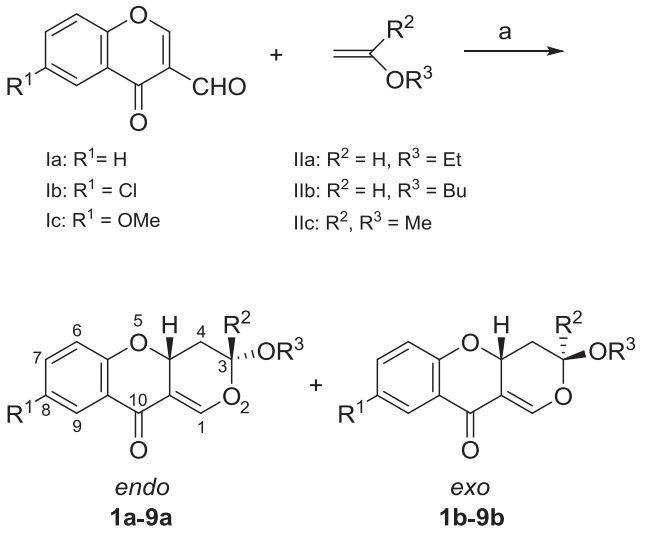

Fig. 1. Synthetic protocol for pyrano[4,3-b][1]benzopyranone derivatives. Reagents and conditions: (a) toluene in a sealed tube, 115 °C.

Table 1
Synthesis of pyrano[4,3-*b*][1]benzopyranone derivatives.

Entry	R^1	R^2	R^3	Cycloadducts		Total yield (%)	Ratio of *endo/exo*
				endo	*exo*		
1	H	H	Et	**1a**	**1b**	91	1.9:1
2	H	H	Bu	**2a**	**2b**	93	1.8:1
3	H	Me	Me	**3a**	**3b**	93	3.8:1
4	Cl	H	Et	**4a**	**4b**	93	2.1:1
5	Cl	H	Bu	**5a**	**5b**	94	1.9:1
6	Cl	Me	Me	**6a**	**6b**	93	3.4:1
7	MeO	H	Et	**7a**	**7b**	89	2.0:1
8	MeO	H	Bu	**8a**	**8b**	96	1.8:1
9	MeO	Me	Me	**9a**	**9b**	89	3.1:1

with sub-micromolar order IC_{50} values similar to pargyline, a positive control. The inhibition of MAO-B by compound **5b** was reversible, whereas pargyline inhibited MAO-B irreversibly (data not shown). Compounds **2a**, **2b**, **4a**, **4b**, **6a**, **6b** and **8b** showed micromolar order IC_{50} values toward MAO-B. Substitution of butoxy at the C3 position or of chlorine at the C8 position on pyrano[4,3-*b*][1]benzopyranone appeared to increase the inhibitory activity toward MAO-B, as can be seen in the comparison of compounds **1** vs. **2**, **4** vs. **5**, **7** vs. **8**, **1** vs. **4**, **2** vs. **5**, and **3** vs. **6**.

2.3. Inhibitory activities of the synthetic compounds toward ChEs

As can be seen in Table 2, most of the compounds showed no inhibitory activity to ChEs, although compounds **2a**, **5a**, and **6a** slightly inhibited AChE activity and compounds **2a**, **2b**, **5b**, and **8b** slightly inhibited BChE activity. These results suggest that *exo* type and butoxy-containing pyrano[4,3-*b*][1]benzopyranones may be useful for recognizing BChE, with the exception of compound **2a**. Compound **5b** showed potent MAO-B and weak but distinct BChE inhibitory activities.

2.4. Molecular docking study for calculating the binding energies of compounds to MAO-B

In an effort to elucidate the mechanism by which compound **5b** exhibits potent and selective inhibitory activity toward MAO-B,

Table 2
IC_{50} values of pyrano[4,3-*b*][1]benzopyranone derivatives for MAO-A, MAO-B, AChE and BChE.

Compd.	MAO-A IC_{50} (μM)	MAO-B IC_{50} (μM)	SI	AChE IC_{50} (μM)	BChE IC_{50} (μM)
1a	53	> 100	–	> 100	> 100
1b	35	35	–	> 100	> 100
2a	95	1.2	79	67	44
2b	25	3.2	7.8	> 100	20
3a	28	68	–	> 100	> 100
3b	34	34	–	> 100	> 100
4a	29	1.5	19	> 100	> 100
4b	33	1.7	19	> 100	> 100
5a	84	0.54	160	76	> 100
5b	> 100	0.20	> 500	> 100	21
6a	7.7	2.8	2.8	51	> 100
6b	38	1.7	22	> 100	> 100
7a	15	21	–	94	> 100
7b	19	21	–	> 100	> 100
8a	25	0.39	64	> 100	> 100
8b	4.3	1.3	3.3	> 100	27
9a	19	40	–	> 100	> 100
9b	14	6.8	2.1	> 100	> 100
PC	4.6	0.22	21	0.20	7.1

The selectivity index (SI) is the selectivity for MAO-B and is given as the ratio of IC_{50} value for MAO-A/ IC_{50} value for MAO-B.

molecular docking of compound **5b** into the ligand binding model site of MAO-B was examined using a binding model based on the MAO-B complex structure (6FVZ. pdb) and compared with the binding model of compound **1b**. Though the binding poses of **1b** indicated the space between ligand and protein around Pro104, the chlorine derivative **5b** could fill to that space. On the other hand, the space around Tyr398 was filled by longer sidechain (buthoxy group). The binding score of ligands and MAO-B might be influenced by these factors and chlorine and buthoxy derivative (**5b**) showed more stable energy (**5b**: −9.51 kcal/mol, **1b**: −8.60 kcal/mol). This result was significantly corresponding to MAO-B inhibitory activities.

Thull and Testa [21] reported that tricyclic compounds, such as anthraquinone, xanthene, xanthone, thioxanthone and acridine, selectively inhibit MAO-A activity. Harfenist et al. [22,23] reported that tricyclic *N*-arylamide derivatives also inhibit MAO-A activity selectively. In contrast, many chromone and chromanone derivatives, such as flavones and homoisoflavoninds, inhibit MAO-B activity selectively [8–11]. The active site structures of human MAO-A and MAO-B were recently reported [4,5] and show that MAO-B has a bipartite hydrophobic cavity comprising an entrance cavity and a substrate cavity. The substrate cavity in MAO-B has a volume of ~430 A^3 and the entrance cavity has a volume of ~290 $Å^3$. The combined volume of the two cavities is ~700 $Å^3$ when the gating Ile 199 is in the open conformation. The active site of MAO-A differs from that of MAO-B in that it has a monopartite cavity with a total volume of ~550 $Å^3$. It therefore appears that MAO-B recognizes larger substrates and less stringently than does MAO-A. Consequently, **5b** might be more selective for MAO-B.

3. Conclusion

A series of pyrano[4,3-*b*][1]benzopyranone derivatives (**1a**-**9b**) were synthesized and their SARs were evaluated with respect to MAO-A, MAO-B, AChE, and BChE inhibitory activities. This is the first report identifying pyrano[4,3-*b*][1]benzopyranone derivatives as MAO-B inhibitors. 3-Butoxy-8-chloro-pyrano[4,3-*b*][1]benzopyranone (**5b**) may be useful as a hit compound for the development of novel MAO-B inhibitors.

4. Experimental

4.1. Chemistry

All reagents and solvents were purchased from commercial sources. 3-Formylchromone and 6-chloro-3-formylchromone were purchased from Tokyo Kasei Industry, Tokyo, Japan. 6-Methoxy-3-formylchromone was synthesized according to a previously described method [24]. Analytical thin-layer chromatography was performed on silica-coated plates (silica gel 60F-254; Merck Ltd., Tokyo, Japan) and visualized under UV light. Column chromatography was carried out using silica gel (Wakogel C-200; Wako Pure Chemical Industry Co., Tokyo, Japan). All melting points were determined using a Yanagimoto micro-hot stage and are uncorrected. ^{1}H NMR and ^{13}C NMR spectra were recorded on a Varian 400-MR spectrometer using tetramethylsilane as an internal standard. MS spectra were measured using a JEOL JMS-700 spectrometer. Elemental analyses were carried out on a Yanaco CHN MT-6 elemental analyzer.

4.2. General procedure for preparing pyrano[4,3-b][1]benzopyran derivatives (1-9)

The cycloadducts (**1**-**9**) were synthesized by modifying a previously reported procedure [15]. A mixture of the corresponding 3-formylchromone (**I**, 2 mmol), the appropriate enol ether (**II**, 40 mmol), and toluene (5 mL) was heated at 115 °C for 2–8 h in a sealed tube. The solvent was evaporated under reduced pressure. The residue was purified by silica gel column chromatography (hexane:AcOEt = 10:1) to give the title compound. Satisfactory yields were obtained in all cases and all products were formed as both *endo* and *exo* type adducts, with *endo* predominating (see Table 1).

4.2.1. 3-Ethoxy-4,4a-dihydro-3H,10H-pyrano[4,3-b][1]benzopyran-10-ones (1a and 1b)

Reaction time: 4 h. Total yield (**1a** and **1b**): 91%. Ratio of *endo*:*exo* = 1.9:1.

The *endo* adduct (**1a**): colorless crystal. mp 186–187 °C (lit. 176–177 °C[15]). ^{1}H NMR ($CDCl_3$, 400 MHz) δ: 7.95 (1H, dd, *J* = 7.8, 1.7 Hz, H-9), 7.57 (1H, d, *J* = 1.2 Hz, H-1), 7.45 (1H, ddd, *J* = 8.3, 7.1, 1.7 Hz, H-7), 7.05 (1H, ddd, *J* = 7.8, 7.1, 1.1 Hz, H-8), 6.94 (1H, dd, *J* = 8.3, 1.1 Hz, H-6), 5.24–5.16 (2H, m, H-3 and H-4α), 4.04 (1H, dq, *J* = 9.4, 7.1 Hz, OCH_2), 3.69 (1H, dq, *J* = 9.4, 7.1 Hz, OCH_2), 2.59 (1H, ddd, *J* = 13.1, 6.7, 2.1 Hz, H-4β), 2.33 (1H, dt, *J* = 13.1, 10.0 Hz, H-4α), 1.30 (3H, t, *J* = 7.6 Hz, CH_3). MS (EI) *m/z*: 246 $[M]^+$. The ^{1}H NMR spectrum was similar to that previously reported [15].

The *exo* adduct (**1b**): pale yellow thin crystal. mp 84–85 °C (lit. 83–84 °C[15]). ^{1}H NMR ($CDCl_3$, 400 MHz) δ: 7.96 (1H, dd, *J* = 7.8, 1.8 Hz, H-9), 7.54 (1H, d, *J* = 1.6 Hz, H-1), 7.45 (1H, ddd, *J* = 8.3, 7.1, 1.8 Hz, H-7), 7.05 (1H, ddd, *J* = 7.8, 7.1, 1.0 Hz, H-8), 6.94 (1H, dd, *J* = 8.3, 1.0 Hz, H-6), 5.32 (1H, br t, *J* = 2.5 Hz, H-3), 5.20 (1H, ddd, *J* = 10.5, 6.5, 1.6 Hz, H-4a), 3.86 (1H, dq, *J* = 9.6, 7.1 Hz, OCH_2), 3.62 (1H, dq, *J* = 9.6, 7.1 Hz, OCH_2), 2.55 (1H, ddd, *J* = 13.0, 6.5, 2.3 Hz, H-4β), 2.19 (1H, ddd, *J* = 13.0, 10.5, 2.9 Hz, H-4α), 1.20 (3H, t, *J* = 7.1 Hz, CH_3). MS (EI) *m/z*: 246 $[M]^+$. The ^{1}H NMR spectrum was similar to that previously reported [15].

4.2.2. 3-Butoxy-4,4a-dihydro-3H,10H-pyrano[4,3-b][1]benzopyran-10-ones (2a and 2b)

Reaction time: 2 h. Total yield (**2a** and **2b**): 93%. Ratio of *endo*:*exo* = 1.8:1.

The *endo* adduct (**2a**): colorless crystal. mp 125–126 °C (lit. 120–121 °C [15]). ^{1}H NMR ($CDCl_3$, 400 MHz) δ: 7.94 (1H, dd, *J* = 7.8, 1.8 Hz, H-9), 7.57 (1H, d, *J* = 1.2 Hz, H-1), 7.45 (1H, ddd, *J* = 8.3, 7.1, 1.8 Hz, H-7), 7.05 (1H, ddd, *J* = 7.8, 7.1, 1.0 Hz, H-8), 6.94 (1H, dd, *J* = 8.3, 1.0 Hz, H-6), 5.22–5.16 (2H, m, 3-H and H-4a), 3.97 (1H, dq, *J* = 9.5, 6.7 Hz, OCH_2), 3.60 (1H, dq, *J* = 9.5, 6.7 Hz, OCH_2), 2.59 (1H, ddd, *J* = 13.1, 6.7, 2.1 Hz, H-4β), 2.33 (1H, dq, *J* = 13.1, 10.0 Hz, H-4α), 1.68–1.58 (2H, m, CH_2), 1.46–1.36 (2H, m, CH_2), 0.94 (3H, t, *J* = 7.1 Hz, CH_3). MS (EI) *m/z*: 274 $[M]^+$. The ^{1}H NMR spectrum was similar to that previously reported [15].

The *exo* adduct (**2b**): yellow thin crystal. mp 50–51 °C (lit. 50–51 °C [15]). . Epub 2005 Jul 27H NMR ($CDCl_3$, 400 MHz) δ: 7.97 (1H, dd, *J* = 8.0, 1.8 Hz, H-9), 7.54 (1H, d, *J* = 1.6 Hz, H-1), 7.45 (1H, ddd, *J* = 8.3, 7.1, 1.8 Hz, H-7), 7.05 (1H, ddd, *J* = 8.0, 7.1, 1.1 Hz, H-8), 6.94 (1H, dd, *J* = 8.3, 1.1 Hz, H-6), 5.30 (1H, br t, *J* = 2.5 Hz, H-3), 5.20 (1H, ddd, *J* = 10.5, 6.5, 1.6 Hz, H-4a), 3.80 (1H, dq, *J* = 9.5, 6.6 Hz, OCH_2), 3.55 (1H, dq, *J* = 9.5, 6.6 Hz, OCH_2), 2.55 (1H, ddd, *J* = 13.0, 6.5, 2.3 Hz, H-4β), 2.18 (1H, ddd, *J* = 13.0, 10.5, 2.9 Hz, H-4α), 1.58–1.50 (2H, m, CH_2), 1.38–1.28 (2H, m, CH_2), 0.90 (3H, t, *J* = 7.3 Hz, CH_3). MS (EI) *m/z*: 274 $[M]^+$. The ^{1}H NMR spectrum was similar to that previously reported [15].

4.2.3. 3-Methoxy-3-methyl-4,4a-dihydro-3H,10H-pyrano[4,3-b][1]benzopyran-10-ones (3a and 3b)

Reaction time: 3 h. Total yield (**3a** and **3b**): 94%. Ratio of *endo*:*exo* = 3.8:1.

The *endo* adduct (**3a**): pale yellow crystal. mp 116–117 °C (lit. 114–115 °C [15]). . Epub 2005 Jul 27H NMR ($CDCl_3$, 400 MHz) δ: 7.97 (1H, dd, *J* = 7.9, 1.8 Hz, H-9), 7.58 (1H, d, *J* = 1.4 Hz, H-1), 7.45 (1H, ddd, *J* = 8.3, 7.1, 1.8 Hz, H-7), 7.06 (1H, ddd, *J* = 7.9, 7.1, 1.1 Hz, H-8), 6.96 (1H, dd, *J* = 8.3, 1.1 Hz, H-6), 5.08 (1H, ddd, *J* = 8.7, 6.7, 1.4 Hz, H-4a), 3.43 (3H, s, OCH_3), 2.49 (1H, dd, *J* = 13.2, 8.7 Hz, H-4β), 2.36 (1H, dd, *J* = 13.2, 6.7 Hz, H-4α), 1.49 (3H, s, CH_3). MS (EI) *m/z*: 246 $[M]^+$. The ^{1}H NMR spectrum was similar to that previously

reported [15].

The *exo* adduct (**3b**): colorless crystal. mp 132–133 °C (lit. 127–128 °C [15]). ^{1}H NMR ($CDCl_3$, 400 MHz) δ: 7.96 (1H, dd, *J* = 7.9, 1.7 Hz, H-9), 7.52 (1H, d, *J* = 1.5 Hz, H-1), 7.44 (1H, ddd, *J* = 8.3, 7.1, 1.7 Hz, H-7), 7.04 (1H, ddd, *J* = 7.9, 7.1, 1.0 Hz, H-8), 6.94 (1H, dd, *J* = 8.3, 1.0 Hz, H-6), 5.18 (1H, ddd, *J* = 10.6, 6.7, 1.5 Hz, H-4a), 3.30 (3H, s, OCH_3), 2.58 (1H, dd, *J* = 12.9, 6.7 Hz, H-4β), 2.08 (1H, dd, *J* = 12.9, 10.6 Hz, H-4α), 1.59 (3H, s, CH_3). MS (EI) *m/z*: 246 $[M]^+$. The ^{1}H NMR spectrum was similar to that previously reported [15].

4.2.4. 8-Chloro3-ethoxy-4,4a-dihydro-3H,10H-pyrano[4,3-b][1] benzopyran-10-ones (4a and 4b)

Reaction time: 4 h. Total yield (**4a** and **4b**): 93%. Ratio of *endo*:*exo* = 2.1:1.

The *endo* adduct (**4a**): yellow thin crystal. mp 186–187 °C ^{1}H NMR ($CDCl_3$, 400 MHz) δ: 7.90 (1H, d, *J* = 2.7 Hz, H-9), 7.58 (1H, d, *J* = 1.3 Hz, H-1), 7.38 (1H, dd, *J* = 8.7, 2.7 Hz, H-7), 6.91 (1H, d, *J* = 8.7 Hz, H-6), 5.22 (1H, dd, *J* = 9.9, 2.1 Hz, H-3), 5.17 (1H, ddd, *J* = 9.9, 6.7, 1.3 Hz, H-4a), 4.03 (1H, dq, *J* = 9.5, 7.1 Hz, OCH_2), 3.69 (1H, dq, *J* = 9.5, 7.1 Hz, OCH_2), 2.59 (1H, ddd, *J* = 13.1, 6.7, 2.1 Hz, H-4β), 2.32 (1H, dt, *J* = 13.1, 9.9 Hz, H-4α), 1.30 (3H, t, *J* = 7.1 Hz, CH_3). ^{13}C NMR ($CDCl_3$, 100 MHz) δ: 180.0, 159.1, 152.3, 135.0, 127.5, 126.7, 123.6, 119.4, 111.0, 100.6, 70.7, 65.7, 33.4, 15.0. MS (EI) *m/z*: 280 $[M]^+$. *Anal.* Calcd for $C_{14}H_{13}ClO_4$: C, 59.90; H, 4.67. Found: C, 60.11; H, 4.72.

The *exo* adduct (**4b**): colorless thin crystal. mp 129–130 °C. ^{1}H NMR ($CDCl_3$, 400 MHz) δ: 7.91 (1H, d, *J* = 2.7 Hz, H-9), 7.55 (1H, d, *J* = 1.6 Hz, H-1), 7.38 (1H, dd, *J* = 8.9, 2.7 Hz, H-7), 6.90 (1H, d, *J* = 8.9 Hz, H-6), 5.33 (1H, br t, *J* = 2.4 Hz, H-3), 5.19 (1H, ddd, *J* = 10.5, 6.5, 1.6 Hz, H-4a), 3.86 (1H, dq, *J* = 9.6, 7.1 Hz, OCH_2), 3.62 (1H, dq, *J* = 9.6, 7.1 Hz, OCH_2), 2.55 (1H, ddd, *J* = 13.0, 6.5, 2.2 Hz, H-4β), 2.18 (1H, ddd, *J* = 13.0, 10.5, 2.9 Hz, H-4α), 1.21 (3H, t, *J* = 7.1 Hz, CH_3). ^{13}C NMR ($CDCl_3$, 100 MHz) δ: 179.9, 159.3, 150.7, 134.9, 127.3, 126.7, 123.7, 119.4, 111.7, 98.9, 68.3, 65.0, 31.8, 14.9. MS (EI) *m/z* 280 $[M]^+$. *Anal.* Calcd for $C_{14}H_{13}ClO_4$: C, 59.90; H, 4.67. Found: C, 59.73; H, 4.65.

4.2.5. 3-Butoxy-8-chloro-4,4a-dihydro-3H,10H-pyrano[4,3-b][1] benzopyran-10-ones (5a and 5b)

Reaction time: 4 h. Total yield (**5a** and **5b**): 94%. Ratio of *endo*:*exo* = 1.9:1.

The *endo* adduct (**5a**): colorless crystal. mp 152–153 °C. ^{1}H NMR ($CDCl_3$, 400 MHz) δ: 7.90 (1H, d, *J* = 2.7 Hz, H-9), 7.58 (1H, d, *J* = 1.3 Hz, H-1), 7.38 (1H, dd, *J* = 8.8, 2.7 Hz, H-7), 6.90 (1H, d, *J* = 8.8 Hz, H-6), 5.20 (1H, dd, *J* = 9.9, 2.1 Hz, H-3), 5.17 (1H, ddd, *J* = 9.9, 6.7, 1.3 Hz, H-4a), 3.98 (1H, dt, *J* = 9.5, 6.7 Hz, OCH_2), 3.61 (1H, dt, *J* = 9.5, 6.7 Hz, OCH_2), 2.58 (1H, ddd, *J* = 13.1, 6.7, 2.1 Hz, H-4β), 2.32 (1H, dt, *J* = 13.1, 9.9 Hz, H-4α), 1.67–1.59 (2H, m, CH_2), 1.46–1.36 (2H, m, CH_2), 0.94 (3H, t, *J* = 7.4 Hz, CH_3). ^{13}C NMR ($CDCl_3$, 100 MHz) δ: 180.0, 159.2, 152.3, 135.0, 127.5, 126.7, 123.7, 119.4, 111.0, 100.8, 70.7, 70.0, 33.4, 31.5, 19.1, 13.8. MS (EI) *m/z* 308 $[M]^+$. *Anal.* Calcd for $C_{16}H_{17}ClO_4$: C, 62.24; H, 5.55. Found: C, 62.20; H, 5.58.

The *exo* adduct (**5b**): pale yellow crystal. mp 96–97 °C. ^{1}H NMR ($CDCl_3$, 400 MHz) δ: 7.91 (1H, d, *J* = 2.7 Hz, H-9), 7.55 (1H, d, *J* = 1.6 Hz, H-1), 7.38 (1H, dd, *J* = 8.8, 2.7 Hz, H-7), 6.90 (1H, d, *J* = 8.8 Hz, H-6), 5.31 (1H, br t, *J* = 2.6 Hz, H-3), 5.18 (1H, ddd, *J* = 10.5, 6.5, 1.6 Hz, H-4a), 3.80 (1H, dt, *J* = 9.5, 6.6 Hz, OCH_2), 3.56 (1H, dt, *J* = 9.5, 6.6 Hz, OCH_2), 2.55 (1H, ddd, *J* = 13.0, 6.5, 2.2 Hz, H-4β), 2.18 (1H, ddd, *J* = 13.0, 10.5, 2.9 Hz, H-4α), 1.58–1.50 (2H, m, CH_2), 1.38–1.28 (2H, m, CH_2), 0.90 (3H, t, *J* = 7.4 Hz, CH_3). ^{13}C NMR ($CDCl_3$, 100 MHz) δ: 179.9, 159.3, 150.7, 134.9, 127.3, 126.7, 123.7, 119.4, 111.7, 99.1, 69.3, 68.3, 31.8, 31.4, 19.2, 13.8. MS (EI) *m/z*: 308 $[M]^+$. *Anal.* Calcd for $C_{16}H_{17}ClO_4$: C, 62.24; H, 5.55. Found: C, 62.12; H, 5.36.

4.2.6. 8-Chloro-3-methoxy-3-methyl-4,4a-dihydro-3H,10H-pyrano[4,3-b][1]- benzopyran-10-ones (6a and 6b)

Reaction time: 4 h. Total yield (**6a** and **6b**): 93%. Ratio of *endo*:*exo* = 3.4:1.

The *endo* adduct (**6a**): pale yellow crystal. mp 152–153 °C. ^{1}H NMR ($CDCl_3$, 400 MHz) δ: 7.92 (1H, d, *J* = 2.7 Hz, H-9), 7.60 (1H, d, *J* = 1.4 Hz, H-1), 7.39 (1H, dd, *J* = 8.7, 2.7 Hz, H-7), 6.92 (1H, d, *J* = 8.7 Hz, H-6), 5.06 (1H, ddd, *J* = 8.6, 6.7, 1.4 Hz, H-4a), 3.43 (3H, s, OCH_3), 2.48 (1H, dd, *J* = 13.3, 8.6 Hz, H-4β), 2.35 (1H, dd, *J* = 13.3, 6.7 Hz, H-4α), 1.49 (3H, s, CH_3). ^{13}C NMR ($CDCl_3$, 100 MHz) δ: 180.2, 159.2, 152.4, 134.9, 127.4, 126.7, 123.8, 119.4, 110.0, 104.0, 71.0, 50.1, 35.7, 22.6. MS (EI) *m/z*: 280 $[M]^+$. *Anal.* Calcd for $C_{14}H_{13}ClO_4$: C, 59.90; H, 4.67. Found: C, 59.64; H, 4.62.

The *exo* adduct (**6b**): colorless crystal. mp 148–150 °C. ^{1}H NMR ($CDCl_3$, 400 MHz) δ: 7.91 (1H, d, *J* = 2.7 Hz, H-9), 7.53 (1H, d, *J* = 1.5 Hz, H-1), 7.37 (1H, dd, *J* = 8.8, 2.7 Hz, H-7), 6.90 (1H, d, *J* = 8.8 Hz, H-6), 5.17 (1H, ddd, *J* = 10.6, 6.7, 1.5 Hz, H-4a), 3.30 (3H, s, OCH_3), 2.58 (1H, dd, *J* = 12.9, 6.7 Hz, H-4β), 2.08 (1H, dd, *J* = 12.9, 10.6 Hz, H-4α), 1.60 (3H, s, CH_3). ^{13}C NMR ($CDCl_3$, 100 MHz) δ: 180.0, 159.4, 150.7, 134.9, 127.2, 126.7, 123.7, 119.4, 111.6, 102.9, 69.7, 49.7, 37.3, 22.2. MS (EI) *m/z*: 280 $[M]^+$. *Anal.* Calcd for $C_{14}H_{13}ClO_4$: C, 59.90; H, 4.67. Found: C, 59.90; H, 4.43.

4.2.7. 3-Ethoxy-4,4a-dihydro-8-methoxy-3H,10H-pyrano[4,3-b][1] benzopyran-10-ones (7a and 7b)

Reaction time: 8 h. Total yield (**7a** and **7b**): 89%. Ratio of *endo*:*exo* = 2.0:1.

The *endo* adduct (**7a**): pale yellow thin crystal. mp 166–167 °C (lit. 159–161 °C [15]). ^{1}H NMR ($CDCl_3$, 400 MHz) δ: 7.55 (1H, d, *J* = 1.3 Hz, H-1), 7.38 (1H, d, *J* = 3.2 Hz, H-9), 7.05 (1H, dd, *J* = 9.0, 3.2 Hz, H-7), 6.89 (1H, d, *J* = 9.0 Hz, H-6), 5.20 (1H, dd, *J* = 9.9, 2.1 Hz, H-3), 5.14 (1H, ddd, *J* = 9.9, 6.7, 1.3 Hz, H-4a), 4.04 (1H, dq, *J* = 9.6, 7.2 Hz, OCH_2), 3.81 (3H, s, OCH_3), 3.69 (1H, dq, *J* = 9.6, 7.2 Hz, OCH_2), 2.57 (1H, ddd, *J* = 13.1, 6.7, 2.1 Hz, H-4β), 2.31 (1H, dt, *J* = 13.1, 9.9 Hz, H-4α), 1.30 (3H, t, *J* = 7.1 Hz,). MS (EI) *m/z*: 276 $[M]^+$. The ^{1}H NMR spectrum was similar to that previously reported [15].

The *exo* adduct (**7b**): yellow solid. mp 88–90 °C (lit. 83–84 °C [15]). ^{1}H NMR ($CDCl_3$, 400 MHz) δ: 7.54 (1H, d, *J* = 1.6 Hz, H-1), 7.40 (1H, d, *J* = 3.2 Hz, H-9), 7.05 (1H, dd, *J* = 8.9, 3.2 Hz, H-7), 6.88 (1H, d, *J* = 8.9 Hz, H-6), 5.31 (1H, br t, *J* = 2.6 Hz, H-3), 5.14 (1H, ddd, *J* = 10.4, 6.5, 1.6 Hz, H-4a), 3.86 (1H, dq, *J* = 9.6, 7.1 Hz, OCH_2), 3.81 (3H, s, OCH_3), 3.62 (1H, dq, *J* = 9.6, 7.1 Hz, OCH_2), 2.53 (1H, ddd, *J* = 13.0, 6.5, 2.4 Hz, H-4β), 2.18 (1H, ddd, *J* = 13.0, 10.4, 2.9 Hz, H-4α), 1.20 (3H, t, *J* = 7.1 Hz, CH_3). MS (EI) *m/z*: 276 $[M]^+$. The ^{1}H NMR spectrum was similar to that previously reported [15].

4.2.8. 3-Butoxy-4,4a-dihydro-8-methoxy-3H,10H-pyrano[4,3-b][1] benzopyran-10-ones (8a and 8b)

Reaction time: 4 h. Total yield (**8a** and **8b**): 96%. Ratio of *endo*:*exo* = 1.8:1.

The *endo* adduct (**8a**): pale yellow crystal. mp 112–113 °C. ^{1}H NMR ($CDCl_3$, 400 MHz) δ: 7.57 (1H, d, *J* = 1.3 Hz, H-1), 7.38 (1H, d, *J* = 3.2 Hz, H-9), 7.05 (1H, dd, *J* = 9.0, 3.2 Hz, H-7), 6.88 (1H, d, *J* = 9.0 Hz, H-6), 5.18 (1H, dd, *J* = 10.0, 2.1 Hz, H-3), 5.14 (1H, ddd, *J* = 10.0, 6.7, 1.3 Hz, H-4a), 3.97 (1H, dt, *J* = 9.4, 6.7 Hz, OCH_2), 3.82 (3H, s, OCH_3), 3.60 (1H, dt, *J* = 9.4, 6.7 Hz, OCH_2), 2.57 (1H, ddd, *J* = 13.1, 6.7, 2.1 Hz, H-4β), 2.31 (1H, dt, *J* = 13.1, 10.0 Hz, H-4α), 1.68–1.60 (2H, m, CH_2), 1.46–1.36 (2H, m, CH_2), 0.95 (3H, t, *J* = 7.4 Hz, CH_3). ^{13}C NMR ($CDCl_3$, 100 MHz) δ: 181.0, 155.1, 154.4, 151.5, 123.8, 122.7, 118.8, 111.5, 107.9, 100.6, 70.4, 69.7, 55.7, 33.3, 31.3, 19.0, 13.6. MS (EI) *m/z*: 304 $[M]^+$. *Anal.* Calcd for $C_{17}H_{20}O_5$: C, 67.09; H, 6.62. Found: C, 67.22; H, 6.60.

The *exo* adduct (**8b**): yellow oil. ^{1}H NMR ($CDCl_3$, 400 MHz) δ: 7.55 (1H, d, *J* = 1.6 Hz, H-1), 7.40 (1H, d, *J* = 3.2 Hz, H-9), 7.05 (1H, dd, *J* = 9.0, 3.2 Hz, H-7), 6.88 (1H, d, *J* = 9.0 Hz, H-6), 5.30 (1H, br t,

J = 2.6 Hz, H-3), 5.14 (1H, ddd, J = 10.5, 6.5, 1.6 Hz, H-4a), 3.82 (3H, s, OCH_3), 3.80 (1H, dt, J = 9.5, 6.5 Hz, OCH_2), 3.55 (1H, dt, J = 9.5, 6.5 Hz, OCH_2), 2.53 (1H, ddd, J = 13.0, 6.5, 2.2 Hz, H-4β), 2.17 (1H, ddd, J = 13.0, 10,5, 2.9 Hz, H-4α), 1.58–1.20 (2H, m, CH_2), 1.38–1.30 (2H, m, CH_2), 0.90 (3H, t, J = 7.4 Hz, CH_3). ^{13}C NMR ($CDCl_3$, 100 MHz) δ: 181.0, 155.4, 154.4, 150.0, 123.9, 122.9, 119.0, 112.4, 108.0, 99.0, 69.1, 68.0, 55.8, 31.9, 31.4, 19.2, 13.8. MS (EI) m/z 304 $[M]^+$.

4.2.9. 3,8-Dimethoxy-3-methyl-4,4a-dihydro-3H,10H-pyrano[4,3-b][1] benzopyran-10-ones (9a and 9b)

Reaction time: 4 h. Total yield (**9a** and **9b**): 89%. Ratio of *endo*:*exo* = 3.1:1.

The *endo* adduct (**9a**): yellow solid. mp 93–95 °C. ^{1}H NMR ($CDCl_3$, 400 MHz) δ: 7.58 (1H, d, J = 1.4 Hz, H-1), 7.40 (1H, d, J = 3.2 Hz, H-9), 7.06 (1H, dd, J = 9.0, 3.2 Hz, H-7), 6.90 (1H, d, J = 9.0 Hz, H-6), 5.03 (1H, ddd, J = 8.6, 6.7, 1.4 Hz, H-4a), 3.82 (3H, s, OCH_3), 3.43 (3H, s, OMe), 2.48 (1H, dd, J = 13.2, 8.6 Hz, H-4β), 2.34 (1H, dd, J = 13.2, 6.7 Hz, H-4α), 1.48 (3H, s, CH_3). ^{13}C NMR ($CDCl_3$, 100 MHz) δ: 181.3, 155.3, 154.5, 151.8, 124.0, 122.9, 119.0, 110.6, 108.1, 103.9, 70.6, 55.8, 50.0, 35.7, 22.7. MS (EI) m/z: 276 $[M]^+$. *Anal.* Calcd for $C_{15}H_{16}O_5$: C, 65.21; H, 5.84. Found: C, 64.99; H, 5.79.

The *exo* adduct (**9b**): yellow thin crystal. 107–108 °C. ^{1}H NMR ($CDCl_3$, 400 MHz)δ: 7.52 (1H, d, J = 1.5 Hz, H-1), 7.39 (1H, d, J = 3.2 Hz, H-9), 7.04 (1H, dd, J = 9.0, 3.2 Hz, H-7), 6.88 (1H, d, J = 9.0 Hz, H-6), 5.12 (1H, ddd, J = 10.6, 6.7, 1.5 Hz, H-4a), 3.82 (3H, s, OCH_3), 3.29 (3H, s, OCH_3), 2.56 (1H, dd, J = 12.9, 6.7 Hz, H-4β), 2.06 (1H, dd, J = 12.9, 10.6 Hz, H-4α), 1.59 (3H, s, CH_3). ^{13}C NMR ($CDCl_3$, 100 MHz) δ: 181.2, 155.5, 154.3, 150.1, 123.9, 122.9 119.0, 112.3, 108.0, 102.7, 69.3, 55.8, 49.6, 37.5, 22.3. MS (EI) m/z: 276 $[M]^+$. *Anal.* Calcd for $C_{15}H_{16}O_5$: C, 65.21; H, 5.84. Found: C, 65.24; H, 5.80.

4.3. Biological assays

Recombinant human monoamine oxidase A (MAO-A), MAO-B, acetylcholinesterase, horse serum butyrylcholinesterase, pargyline and kynuramine were purchased from Sigma-Aldrich Japan Co., Tokyo, Japan. Neostigmine and 5,5-dithiobis(2-nitrobenzoic acid) (DTNB) were purchased from Tokyo Chemical Industry Co., Tokyo, Japan.

4.4. MAO inhibitory assay

MAO inhibitory activity was assayed using the method of Novaroli et al. [25]with minor modifications. Briefly, 140 µL of 0.1 M potassium phosphate buffer (pH 7.4), 8 µL of 0.75 mM kynuramine, and 2 µL of a dimethyl sulfoxide (DMSO) inhibitor solution (final DMSO concentration of 1% (v/v) and final concentrations of the inhibitors of 0 – 100 µM), were preincubated at 37 °C for 10 min. Diluted human recombinant enzyme (50 µL) was then added to obtain a final protein concentration of 0.0075 mg/mL (MAO-A) or 0.015 mg/mL (MAO-B) in the assay mixture. The reaction mixture was further incubated at 37 °C and the reaction was stopped after 20 min by the addition of 75 µL of 2 M NaOH. The product generated by MAO, 4-quinolinol, is fluorescent and was measured at Ex 310 nm/Em 400 nm using a microplate reader (Molecular Devices SPECTRA MAX M2). Each data points of samples were triplicate. The sample solution was replaced with DMSO to provide a negative control and pargyline was used as a positive control. The IC_{50} values were calculated from a line through two points which sandwiched the point of 50% (IC_{50}) by plotting the remained activity (%) related to control (100%) versus the logarithm of the inhibitor concentration to obtain a sigmoidal dose–response curve.

4.5. AChE and BChE inhibitory assays

AChE and BChE inhibitory activities were assayed using the method of Oboh et al. [26] Briefly, 2 µL of pyrano[4,3-*b*][1]benzopyranone derivatives dissolved in DMSO, 6 µL of 0.06 mg/mL acetylthiocholine or 0.12 mg/mL butyrylthiocholine dissolved in 0.1 M phosphate buffer (pH 8.0), 180 µL of the buffer, 6 µL of 0.3 mM DTNB dissolved in the buffer, and 6 µL of 0.15 U/mL AChE or 0.075 U/mL BChE dissolved in the buffer were added and mixed in a 96-well plate. Enzyme activity was determined as the change in absorbance at 412 nm every 5 min during 30 min with a micro-plate reader (Molecular Devices SPECTRA MAX M2). The sample solution was replaced with DMSO as a control. Neostigmine was used as a positive control. The calculations of IC_{50} values were described above.

4.6. Molecular docking study

The MAO-B crystal structure was retrieved from the Protein Data Bank (PDB code: 6FVZ) and imported into the Auto-Dock program (Version 4.2). The structures of compounds **1b** and **5b** were drawn using ChemBioDrawUltra 11.0 and subjected to energy minimization using molecular mechanics (MM2). AutoGrid was used for calculating the grid maps and the grid was centered on the ligand binding site of MAO-B such that it would totally cover the ligand molecule. The centroid of the grid map was set to X: 17, Y: 129, Z: 26, number of grid points X:60 Y:60 Z:70. The maximum number of energy evaluations was set to 250,000. Both ligand and receptor docking were performed using the Lamarckian Genetic Algorithm (Runs 20) after using the default parameter settings generated by AutoDockTools for docking. The calculated binding energies of **1b** and **5b** were the average for each enantiomer.

Acknowledgment

We express our gratitude to Dr. K. Samejima for his help in preparing the manuscript

Appendix A. Supplementary material

Supplementary data to this article can be found online at https://doi.org/10.1016/j.bioorg.2018.11.004.

References

[1] B. Winblad, P. Amouyel, S. Andrieu, C. Ballard, C. Brayne, H. Brodaty, A. Cedazo-Minguez, B. Dubois, D. Edvardsson, H. Feldman, L. Fratiglioni, G.B. Frisoni, S. Gauthier, J. Georges, C. Graff, K. Iqbal, F. Jessen, G. Johansson, L. Jönsson, M. Kivipelto, M. Knapp, F. Mangialasche, R. Melis, A. Nordberg, M.O. Rikkert, C. Qiu, T.P. Sakmar, P. Scheltens, L.S. Schneider, R. Sperling, L.O. Tjernberg, G. Waldemar, A. Wimo, H. Zetterberg, Defeating Alzheimer's disease and other dementias: a priority for European science and society, Lancet Neurol. 15 (5) (2016 Apr) 455–532, https://doi.org/10.1016/S1474-4422(16)00062-4.

[2] P. Williams, A. Sorribas, M.J. Howes, Natural products as a source of Alzheimer's drug leads, Nat. Prod. Rep. 28 (1) (2011 Jan) 48–77, https://doi.org/10.1039/c0np00027b Epub 2010 Nov 12.

[3] A.S. Kalgutkar, N. Castagnoli Jr., Selective inhibitors of monoamine oxidase (MAO-A and MAO-B) as probes of its catalytic site and mechanism, Med. Res. Rev. 15 (4) (1995) 325–388.

[4] D.E. Edmondson, L. De Colibus, C. Binda, M. Li, A. Mattevi, New insights into the structures and functions of human monoamine oxidases A and B, J. Neural Transm. (Vienna) 114 (6) (2007) 703–705 Epub 2007 Mar 29.

[5] L. De Colibus, M. Li, C. Binda, A. Lustig, D.E. Edmondson, A. Mattevi, Three-dimensional structure of human monoamine oxidase A (MAO A): relation to the structures of rat MAO A and human MAO B, Proc. Natl. Acad. Sci. U. S. A. 102 (36) (2005) 12684–12689 Epub 200Aug 29.

[6] G. Ferino, S. Vilar, M.J. Matos, E. Uriarte, E. Cadoni, Curr, Monoamine oxidase inhibitors: ten years of docking studies, Top. Med. Chem. 12 (20) (2012) 2145–2162.

[7] S. Carradori, R. Silvestri, New frontiers in selective human MAO-B inhibitors, J. Med. Chem. 58 (17) (2015 Sep 10) 6717–6732, https://doi.org/10.1021/jm501690r Epub 2015 May 11.

[8] S. Carradori, M. D'Ascenzio, P. Chimenti, D. Secci, A. Bolasco, Selective MAO-B inhibitors: a lesson from natural products, Mol. Divers. 18 (1) (2014) 219–243, https://doi.org/10.1007/s11030-013-9490-6 Epub 2013 Nov 12.

[9] S. Schedin-Weiss, M. Inoue, L. Hromadkova, Y. Teranishi, N.G. Yamamoto, B. Wiehager, N. Bogdanovic, B. Winblad, A. Sandebring-Matton, S. Frykman, L. Tjernberg, O, Monoamine oxidase B is elevated in Alzheimer disease neurons, is

associated with γ-secretase and regulates neuronal amyloid β-peptide levels, Alzheimers Res. Ther. 9 (1) (2017) 57, https://doi.org/10.1186/s13195-017-0279-1.
[10] A. Gaspar, M.J. Matos, J. Garrido, E. Uriarte, F. Borges, Chromone: a valid scaffold in medicinal chemistry, Chem. Rev. 114 (9) (2014) 4960–4992, https://doi.org/10.1021/cr400265z Epub 2014 Feb 21.
[11] S. Emami, Z. Ghanbarimasir, Recent advances of chroman-4-one derivatives: synthetic approaches and bioactivities, Eur. J. Med. Chem. 26 (93) (2015) 539–563, https://doi.org/10.1016/j.ejmech.2015.02.048 Epub 2015 Feb 25.
[12] L. Jalili-Baleh, E. Babaei, S. Abdpour, S. Nasir Abbas Bukhari, A. Foroumadi, A. Ramazani, M. Sharifzadeh, M. Abdollahi, M. Khoobi, A review on flavonoid-based scaffolds as multi-target-directed ligands (MTDLs) for Alzheimer's disease, Eur. J. Med. Chem. 152 (2018) 570–589, https://doi.org/10.1016/j.ejmech.2018.05.004 Epub 2018 May 7.
[13] N. Jiang, A.I. Doseff, E. Grotewold, Flavones: from biosynthesis to health benefits, Plants (Basel) 5 (2) (2016), https://doi.org/10.3390/plants5020027 pii: E27.
[14] K.P. Ko, Isoflavones: chemistry, analysis, functions and effects on health and cancer, Asian Pac. J. Cancer Prev. 15 (17) (2014) 7001–7010.
[15] S.T. Saengchantara, T.W. Wallace, Heterodiene cycloadditions of 3-acylchromones with enol ethers, J. Chem. Soc. Perkin Trans. 1 (1986) 789–794.
[16] S.J. Coutts, T.W. Wallace, Heterodiene cycloadditions: Preparation and transformations of some substituted pyrano[4,3-b][1]benzopyrans, Tetrahedron 50 (40) (1994) 11755–11780.
[17] R. Uddin, A. Zaman, Synthesis of some nitrogen heterocycles from the 3-formylchromone-ethyl-vinyl ether adduct, Indian J. Chem. 34B (1995) 1039–1042.
[18] V.Ya Sosnovskikh, I.A. Khalymbadzha, R.A. Irgashev, P.A. Slepukhin, Stereoselective hetero-Diels-Alder reaction of 3-(polyfluoroacyl)chromones with enol ethers. Novel synthesis of 2-RF-containing nicotinic acid derivatives, Tetrahedron 64 (44) (2008) 10172–10180.
[19] A. Kaur, V. Sharma, A. Budhiraja, H. Kaur, V. Gupta, R. Kant, M.P.S. Ishar, Synthesis and evaluation of substituted 4,4a-dihydro-3H,10H-pyrano[4,3-b][1]benopyran-10-one as antimicrobial agent. ISRN, Med. Chem. (2013) 11 ID 619535.
[20] Junko Nagai, Haixia Shi, Yuka Kubota, Kenjiro Bandow, Noriyuki Okudaira, Yoshihiro Uesawa, Hiroshi Sakagami, Mineko Tomomura, Akito Tomomura, Koichi Takao, Yoshiaki Sugita, Quantitative structure – cytotoxicity relationship of pyrano[4,3-b]chromones, Anticancer Res. 38 (8) (2018) 4449–4457.
[21] U. Thull, B. Testa, Screening of unsubstituted cyclic compounds as inhibitors of monoamine oxidases, Biochem. Pharmacol. 47 (12) (1994 Jun 15) 2307–2310.
[22] S.A.R. Arylamide, M. Harfenist, C.T. Joyner, P.D. Mize, H.L. White, Selective inhibitors of monoamine oxidase, J. Med. Chem. 37 (13) (1994) 2085–2089.
[23] M. Harfenist, D.J. Heuser, C.T. Joyner, J.F. Batchelor, H.L. White, Selective inhibitors of monoamine oxidase. 3. Structure-activity relationship of tricyclics bearing imidazoline, oxadiazole, or tetrazole groups, J. Med. Chem. 39 (9) (1996) 1857–1863.
[24] K. Takao, R. Ishikawa, Y. Sugita, Synthesis and biological evaluation of 3-styrylchromone derivatives as free radical scavengers and α-glucosidase inhibitors, Chem. Pharm. Bull. 62 (8) (2014) 810–815.
[25] L. Novaroli, M. Reist, E. Favre, A. Carotti, M. Catto, P.A. Carrupt, Human recombinant monoamine oxidase B as reliable and efficient enzyme source for inhibitor screening, Bioorg. Med. Chem. 13 (22) (2005) 6212–6217 Epub 2005 Jul 27.
[26] G. Oboh, O.M. Agunloye, A.J. Akinyemi, A.O. Ademiluyi, S.A. Adefegha, Comparative study on the inhibitory effect of caffeic and chlorogenic acids on key enzymes linked to Alzheimer's disease and some pro-oxidant induced oxidative stress in rats' brain-in vitro, Neurochem. Res. 38 (2) (2013) 413–419, https://doi.org/10.1007/s11064-012-0935-6 Epub 2012 Nov 27.